Talanta 175 (2017) 209–216

Contents lists available at ScienceDirect

Talanta

journal homepage: www.elsevier.com/locate/talanta

Electrochemical enzyme biosensors based on calcium phosphate materials for tyramine detection in food samples

Marta Sánchez-Paniagua López, Esther Redondo-Gómez, Beatriz López-Ruiz*

Sección Departamental de Química Analítica. Facultad de Farmacia. Universidad Complutense de Madrid, 28040 Madrid, Spain

ARTICLE INFO

Keywords:
Electrochemical biosensor
Tyrosinase
Calcium phosphate
Tyramine
Cheese

ABSTRACT

Electrochemical tyrosinase biosensors for tyramine determination were developed by the immobilization of the enzyme in calcium phosphate materials (CaPs) followed by cross-linking with glutaraldehyde. Tyramine was detected by the electrochemical reduction at −0.1 V of the o- enzymatically-formed dopaquinone. Three different CaPs were explored as immobilization systems, monetite, brushite and brushite cement. Biosensors based on brushite matrices provide better analytical properties than the monetite one. Compared to brushite, a 10-fold increase of sensitivity was obtained with the brushite cement-based biosensor, which highlights the effect of brushite crystal formation in the presence of the enzyme in the biosensor performance. Several variables involved in the enzyme immobilization method such as glutaraldehyde cross-linking time, PPO/brushite ratio and thickness of the brushite-enzyme film were investigated. Furthermore, the effects of pH and temperature on biosensor performance were also optimized.

Brushite cement-PPO-GA biosensor resulted in a reliable, highly sensitive, fast, inexpensive and easy analytical method for tyramine detection. Under optimal conditions (time of 15 min, a ratio of 1.0 and 50 μg of the brushite-enzyme mixture, 20 °C and pH 6,0), a linear range of 5.8×10^{-7} to 1.6×10^{-5}, sensitivity 1.50×10^{3} mA M^{-1} cm^{-2}, detection limit, 4.85×10^{-8} M and a response time, 6 s were obtained. The suitability of the proposed biosensor to determine the tyramine content in cheese samples has been explored. The mean analytical recovery of added tyramine in gouda and brie cheeses were found to be 95.5 ± 5.8 and 96.9 ± 7.5 respectively. A study of the tyramine content evolution over the course of a week under inadequate storage showed the importance of monitoring the degradation of certain foods.

1. Introduction

Biogenic amines (BA) are organic nitrogenous compounds that are naturally formed in food by bacterial decarboxylation of the corresponding amino acids and participate in numerous metabolic processes in living organisms. The consumption of food containing high concentration of these compounds has a negative impact on human health through direct toxic effects, producing diarrhea, migraine, tachycardia, low blood pressure, etc [1]. Among the foods with the highest content of biogenic amines are fish, vegetables, fermented foods, and beverages. Moreover, within the biogenic amines, the most important are histamine, putrescine, tyramine, cadaverine and β-phenyl ethylamine [2]. Currently, a legislative framework has been established only in the EU to control the limit levels of histamine in different fishery products, i.e. 200 and 400 mg kg^{-1} [3].

The European Food Safety Authority informed that findings of certain levels of toxic biogenic amines in fermented food could be a concerning matter and reported a recent increase of BA content in some fermented foods [4]. Cheese is a fermented dairy food that can accumulate biogenic amines at high concentrations [5], being tyramine the most toxic of them [6,7]. Tyramine, 4-(2-aminoethyl)phenol, is a naturally occurring monoamine compound derived from the amino acid tyrosine by decarboxylation, that could be responsible for the so-called "cheese reaction" which increases blood pressure causing severe migraines and even brain hemorrhages, especially in sensitive individuals [8,9]. Although there is no legislation to limit the content of tyramine in cheese, it is known that the toxicity thresholds are 100–400 mg kg^{-1} of cheese [10,11]. The control of tyramine content in cheese is of great importance, not only due its toxic effects but also because it can be used as an indicator of food quality, given that tyramine levels gradually increase as a consequence of microbial contamination, meaning inappropriate conditions during food processing and storage [12–14].

The development of sensitive and inexpensive methods for the determination of tyramine in different food samples is of paramount importance. Different techniques have been developed for this purpose.

* Corresponding author.
E-mail address: bealopru@ucm.es (B. López-Ruiz).

http://dx.doi.org/10.1016/j.talanta.2017.07.033
Received 25 May 2017; Received in revised form 10 July 2017; Accepted 12 July 2017
Available online 15 July 2017

High performance liquid chromatography, combined with different detection techniques is the most commonly used strategy [15–17]. Moreover, capillary electrophoresis has been reported [18,19]. Quantitative polymerase chain reaction [20,21] has also been described to detect tyramine-producing microorganisms in food samples. However, most of these methods are expensive and require a time-consuming sample pretreatment. Electrochemical biosensors represent interesting alternative for tyramine quantification due to their advantageous analytical properties such as high sensitivity, simplicity, rapidity, selectivity and possibility of miniaturization. Different enzymes and enzyme-immobilizing materials have been reported in the literature regarding the development of enzyme biosensors for tyramine detection, including sol-gel technique [22], polymers [23,24], carbon nanotubes [25] and nanoparticles [26].

The present work focuses on the design and performance of enzyme-based electrochemical biosensors for tyramine detection, using tyrosinase as biological material and ortophosphate calcium materials as enzyme-immobilizing matrices. These inorganic materials have proven to be highly effective enzyme host matrices in biosensing applications [27,28]. The applicability of the proposed biosensor was explored in the detection of tyramine in cheeses and in the evolution of tyramine levels throughout its period of storage.

2. Material and methods

2.1. Reagents

Polyphenol oxidase (PPO, ED 1.14.18.1, tyrosinase from Mushrooms, 1530 Umg^{-1}), tyramine, Tyrosine, phenylalanine, glutamic acid, catechol, β-tricalcium phosphate (β-TCP), monocalcium phosphate anhydrous (MCPA), calcium phosphate anhydrous (monetite), dicalcium phosphate dihydrate (brushite) and glutaraldehyde solution 25% in water were purchased from Sigma-Aldrich (St Louis, MO, USA). Sodium dihydrogen phosphate, disodium hydrogen phosphate, sodium acetate, $CaCl_2$, $MgCl_2$ and $NaNO_3$ were obtained from Panreac (Spain). Phosphate buffer solutions were prepared from sodium monohydrogen and dihydrogen phosphate (Panreac, Spain). Water purified with a Milli-Q system (Millipore, Milford, MA, USA) was used for preparation of aqueous solutions.

2.2. Instrumentation and measurements

Scanning electron micrographs (SEM) of the microparticles were obtained with a JEOL JSM-6400 microscope operating at an acceleration voltage of 20 kV and 5000 magnification. Electrochemical measurements were carried out with a μ-Autolab PGSTAT12 potentiostat with GPES 4.9 software (EcoChemia, The Netherlands), connected to a three-electrode potentiostatic cell with a modified glassy-carbon working electrode (diameter 3 mm), a Pt counter electrode and an Ag/AgCl reference electrode. The working electrode surface was polished with alumina slurry paste (0.05 mm and 0.1 mm) and was rinsed with ethanol and water. All experimental amperometric measurements were carried out in a thermostated cell containing 10 mL of buffer solution. The pHs of buffer solutions were adjusted using a Mettler Toledo MP230 pH meter. The spectrophotometric measurements were performed with a Genesys 10 Spectrophotometer (Thermo Scientific, Spain). The detection limit was obtained following IUPAC recommendation. The response time was determined as the time required to reach the 95% of the steady-state current.

2.3. Matrices for enzyme adsorption

Differents CaPs were studied as host materials for the adsorption of the enzyme; without and with hydration water monetite ($CaHPO_4$), and brushite ($CaHPO_4{\cdot}2H_2O$). Also two immobilization system were tested, a direct addition of PPO on brushite crystals (called brushite) and brushite crystal preparation from the precursors (β-TCP and MCPA) in presence of PPO (called brushite cement) [27].

2.4. Biosensor preparation

CaPs suspensions (2 mg mL^{-1}) were prepared by dispersing monetite, brushite or the brushite cement precursors in deionized water and stirring overnight. A solution of PPO 2 mg mL^{-1} was prepared, and a mixture of CaP and PPO was spread on a glassy carbon electrode surface. The biolayer was left to air-dry at room temperature for 2 h. In order to induce protein cross-linking, the electrode was incubated in a glutaraldehyde saturated atmosphere. Finally, the obtained enzyme/CaP biomembrane was hydrated for 10 min in a 0.1 M PBS pH 6.0. As control, a calcium phosphate free electrode was prepared by drying 12.5 μL of a PPO solution (2 mg mL^{-1}) on the electrode surface and exposing it to glutaraldehyde vapor for 15 min.

2.5. Real samples preparation

Gouda and Brie cheese were acquired in local supermarkets. Samples preparation was carried out according to the procedure described in the literature [29]. 1 g of cheese was accurately weighed and 2 mL of phosphate buffer solution 0.1 M pH 6 was added. The tube containing the sample was mixed in a vortex system for 1 min and then in an ultrasonic bath for 10 min. The mixture was centrifuged for 10 min at 3000 rpm and the supernatant was recovered. The procedure was repeated and the extracts were collected and stored at −20 °C. Addition of 100 μL of the supernatant was placed into the electrochemical cell, containing 10 mL of PBS, current intensity was measured and the concentration of tyramine was calculated. Three replicates were measured.

3. Results and discussion

3.1. Comparison of biosensors based on different CaPs

Monetite, brushite and brushite cement were used as PPO immobilizing systems, in the development of electrochemical biosensors for tyramine detection. As SEM micrographs reveal (Fig. 1A), monetite produces smaller particles than matrices based on brushite materials, and homogeneously distributed over the electrode surface. Comparing the SEM images of brushite (Fig. 1B), and brushite cement (Fig. 1C) larger and more heterogeneously sized particles can be seen in the former where crystal laminates are evident. The use of brushite cement involves the growth of brushite crystal on the electrode surface in presence of PPO. This process could be responsible for the formation of more irregular and smaller crystals than the brushite ones.

Cyclic voltammograms of the electrochemically generated o-dopaquinone were performed, using a solution of tyramine 10 mM in 0.1 M PBS pH 6.0 under stirring and purged with nitrogen, with GCE and calcium phosphate materials modified GCE (Fig. 2A). In order to generate o-dopaquinone electrochemically, before starting the scans, this solution was kept at a fixed potential of 400 mV during 300 s seconds. The relationship between the cathodic peak current and the scan rate was studied in the range of 100–1000 mV s^{-1}. In all cases, a clear reduction peak resulting from the electrochemical reduction of the o-dopaquinone appears. The peak potentials were found to be at −160 mV, −120 mV and −70 mV for monetite, brushite cement and brushite respectively. A smaller oxidation peak was observed at 200 mV for brushite and 150 mV for brushite cement, less pronounced in monetite matrix.

When brushite materials were used, the cathodic peak current was probed to be proportional to the scan rate, characteristic of the adsorption-limited process (Fig. 2B). However, with monetite the cathodic peak current was proportional to the square-root scan rate (Fig. 2C) characteristic of an electrode process controlled by diffusion.

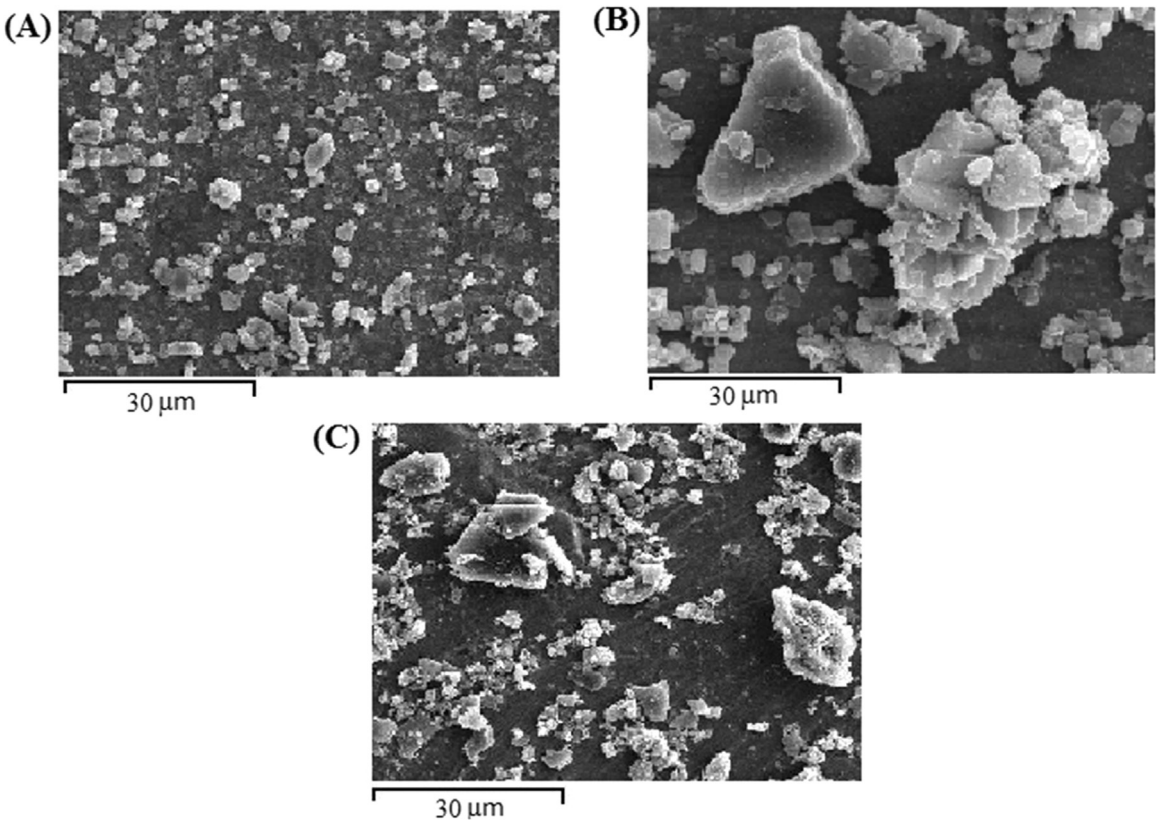

Fig. 1. SEM micrograph of (A) PPO/monetite (1:1, w:w), (B) PPO/brushite (1:1, w-w) and (C) PPO/brushite cement (1:1, w:w).

The weak oxidation peak that appears in monetite matrix could be attributed to the diffusion of the electrochemically reduction product of the o-quinone, from the immobilized layer to the solution. In brushite matrices, this product remains adsorbed in the matrix, giving a greater oxidation signal.

Tyramine was detected by the electrochemical reduction of the o-dopaquinone enzymatically formed at −0.1 V, using the three inorganic materials (PPO/CaPs ratio 1.0; 25 µg of mixture and 15 min of GA). The analytical properties obtained with tyramine solutions (PBS; pH 6.0) and 20 °C are summarized in Table 1. Fig. 3 shows the calibration curves of the biosensors based on inorganic matrices as well as a control biosensor (GCE-PPO).

Enzyme adsorption on CaPs matrixes improves the sensitivity and decreases the detection limit of the biosensor versus the control GCE-PPO biosensor. Great differences in Jmax and in the profile of calibration curves can be seen in Fig. 3. Two distinct behaviors are clearly evidenced, on one hand, among both brushite materials, and, on the other hand, in the monetite and control. Considering that Jmax is related to the amount of available enzyme, i.e. immobilized enzyme on the electrode surface, a spectrophotometric assay to evaluate the immobilization efficiency was carried out [30]. This assay is based on the absorbance at 380 nm of the o-quinones enzymatically generated after catechol addition. Control and modified electrodes were incubated in 1.5 mL of PBS for 10 min. Then, 0.5 mM of catechol was added and the absorbance of these solutions was measured. A solution of PPO of 25 µg (38.25 IU, equal to the amount of PPO placed in the electrode) in 1.5 mL of PBS pH 6.0 was used as reference. The loss of enzyme was 4.0 ± 0.9%, 10.4 ± 1.5%, 24.4 ± 3.1% and 32.8 ± 4.5% for GCE-brushite cement-PPO, GCE-brushite-PPO, GCE-PPO and GCE-monetite-PPO sensors, respectively. As expected, this enzyme loss correlates to the decrease of Jmax observed in Fig. 3.

Referring to the profiles of the calibration curves, biosensor based on brushite cement shows a characteristic profile of a purely kinetic (enzymatic) process, very close to the brushite. These results are in agreement with those obtained by cyclic voltammetry, i.e. the electroactive product enzymatically formed remains adsorbed at the interface electrode/solution, there is no diffusion, and then the limiting process is the enzymatic one. However, when the electroactive product reaches the electrode by diffusion, the diffusion rate is lower than the enzyme reaction rate and the profile does not respond to the characteristic enzymatic profile, as in the case of monetite (Fig. 3).

These results may be attributed to the effect of crosslinking with GA. When the enzyme is more exposed, the contact with GA vapors would result in the formation of excessive intermolecular bonds between the enzyme and the crosslinker, resulting in a very compact network that hinders substrate access to the enzyme. When the CaP material is incorporated as host matrix, less PPO-GA intermolecular bonds are expected since PPO is first inmobilized in the matrix and subsequently crosslinked, generating a less compact network resulting in easier access of the substrate to the active center of the enzyme

Considering the profiles of the calibration curves, brushite matrices exhibit greater Jmax values due to the higher immobilization efficiency. If the enzyme is adsorbed in the brushite matrices, the o-quinone is enzymatically generated in the interface electrode/solution, generating a significant increase in the amperometric response. Likewise, higher slopes were obtained, which points to enzyme kinetics as being the limiting process, whereas diffusion seems to be the limiting process for the monetite. The only difference between both immobilization matrices is the presence of hydration water in brushite materials, which favors the adsorption of hydrosoluble tyrosinase. So, the enzyme will be immersed in these matrices, and therefore, more protected against the GA attack. These results are in agreement with the previously reported showing that enzyme biosensors based on monetite give the best analytical properties in non-aqueous media [31]. The response times obtained with monetite (10 s) and brushite based biosensors (6 s) support the above hypothesis.

Comparing the biosensor responses using brushite cement and brushite, the clear difference in calibration profiles observed could be

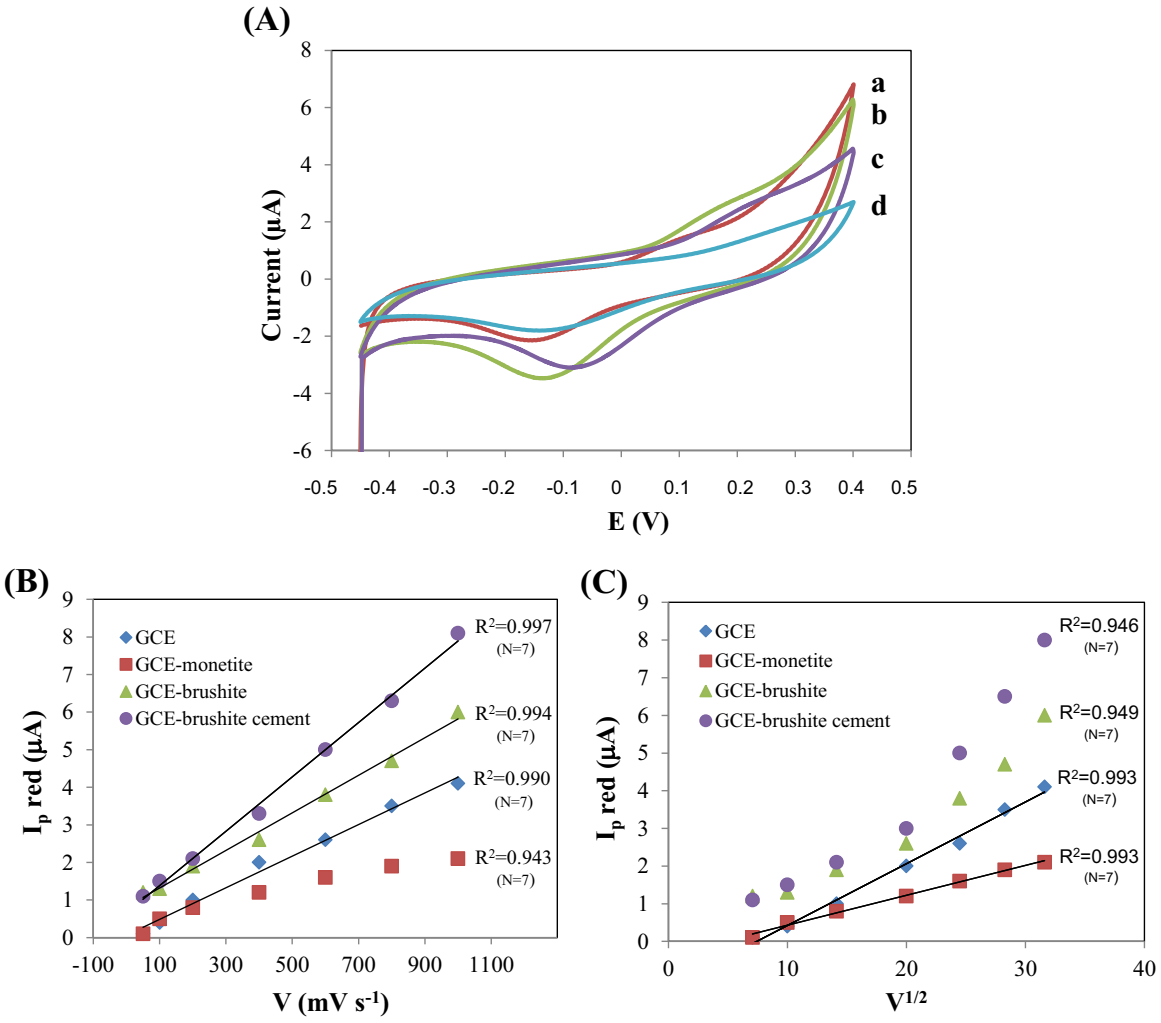

Fig. 2. (A) Cyclic voltammograms of the electrochemically generated o-dopaquinone from a solution of 0.01 M tyramine in a 0.1 M phosphate buffer solution pH 6.0 under nitrogen conditions (kept 300 s at +0.4 V), for (a) GCE-monetite, (b) GCE-brushite cement, (c) GCE-brushite and (d) GCE. Scan rate: 200 mV s^{-1}. Plot of the cathodic peak current for o-dopaquinone versus: (B) the scan rate and (C) the square root of scan rate.

owed to the immobilization systems. In the case of brushite cement crystals growth in presence of PPO, whereas in brushite crystals growth before enzyme immobilization. Thus, most enzyme molecules are probably entrapped within the brushite cement, while in the case of brushite, the enzyme most likely will be adsorbed on the matrix surface. Given that PPO is less 'protected' against crosslinking in later, the profiles and sensitivities obtained (S=1830 mA M^{-1} cm^{-2} versus S=160 mA M^{-1} cm^{-2} for brushite cement and brushite, respectively) could be owed to the higher exposition of the PPO to GA vapors.

3.2. Optimization of PPO/brushite cement based biosensor preparation

According to the results obtained to this point, brushite cement was selected as immobilization matrix, and subsequent optimization of the biosensor for tyramine detection was performed with this inorganic material. Variables affecting the immobilization system and the experimental conditions involved in the response were optimized.

3.2.1. Biosensor composition

3.2.1.1. Enzyme/brushite ratio. This ratio is of great importance to know the optimal amount of inorganic material that guarantees the immobilization of the whole enzyme but does not hinder the diffusion processes involved in the overall process. The amount of brushite crystals on the electrode surface has to be high enough to immobilize the enzyme, but without interfering with the substrate and product diffusion through the matrix.

The enzyme/brushite ratio studied was varied from 0.25 to 2.0,

Table 1
Analytical properties of the biosensors for tyramine detection.

Biosensor	Sensitivity (mA M^{-1} cm^{-2})	Jmax (µA cm^{-2})	Linear range (M)	R^2 (n)	DL (µM)
GCE-PPO-brushite cement	$18.3 \cdot 10^2$	228.9	$3.0 \cdot 10^{-7}$ to $2.5 \cdot 10^{-5}$	0.999 (10)	0.05
GCE-PPO brushite	$1.6 \cdot 10^2$	215.1	$3.0 \cdot 10^{-6}$ to $4.5 \cdot 10^{-4}$	0.998 (11)	3
GCE-PPO-monetite	42.7	90.8	$1.6 \cdot 10^{-5}$ to $1.2 \cdot 10^{-3}$	0.994 (10)	11
GCE-PPO	25.2	137.3	$4.5 \cdot 10^{-5}$ to $3.9 \cdot 10^{-3}$	0.993 (7)	25

Jmax: maximum current density; R: correlation coefficient of the linear range (n: number of points in the linear range); DL: detection limit.

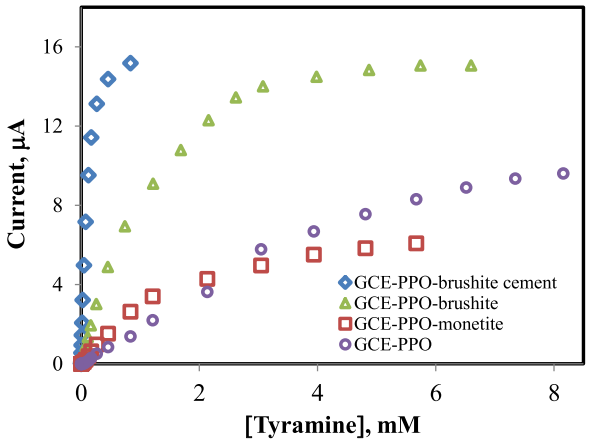

Fig. 3. Calibration curves of the biosensors based on calcium phosphate matrices compared to the control biosensor (GCE-PPO). Experimental conditions: 0.1 M PBS pH 6.0, 20 °C and −0.1 V vs. Ag/AgCl.

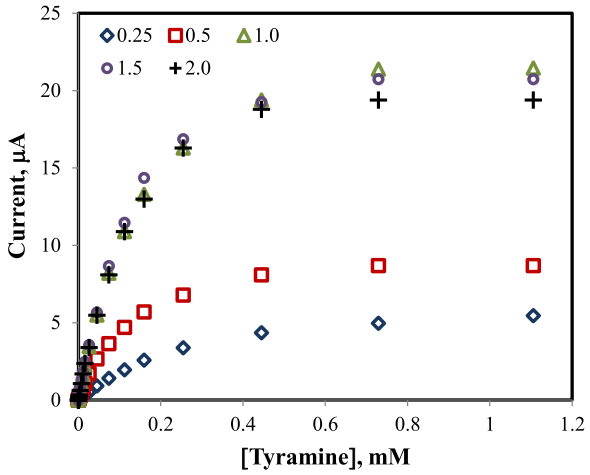

Fig. 4. Influence of enzyme/brushite cement ratio on the biosensor response (50 µg of mixture). Experimental conditions: 0.1 M PBS pH 6.0, 20 °C and −0.1 V vs. Ag/AgCl.

keeping the amount of PPO in the mixture constant at 25 µg, optimum value previously reported [27]. The rest of variables remained constant. Sensitivity and maximum current density increased considerable with increasing enzyme/brushite ratio up to 1.0 (S= $2.75{\cdot}10^2$ µA mM^{-1} cm^{-2} and J_{max}=82.16 µA cm^{-2} for ratio 0.25 and S= $1.99{\cdot}10^3$ µA mM^{-1} cm^{-2} and J_{max}=306.21 µA cm^{-2} for ratio 1.0), plateauing beyond this point (Fig. 4). The lower current density obtained with low enzyme/brushite ratios is due to a diffusional impairment caused by the high amount of brushite deposited on the electrode surface. Greater PPO/brushite ratios than 1.0 did not produce an increase in the current density because the amount of brushite is insufficient to immobilize the entire amount of added enzyme. The presence of enzymatic activity in the buffer solution used to stabilize the electrode confirms this hypothesis. Considering that, the maximum signal was obtained with a PPO/brushite ratio of 1.0 without enzyme loss, this value was chosen for further experiments.

3.2.1.2. Amount of PPO/brushite mixture deposited on the electrode. It is important to study the amount of enzyme/brushite cement spread on the electrode surface because an increase produces higher enzyme quantity in the biosensor but also generates a highly compact layer that could be detrimental to the analytical performance. This experiment was performed varying the amount of both components from 25 to 150 µg, and the ratio was kept constant (1:1). Analytical properties were improved for 50 µg of mixture (S= $2.20{\cdot}10^3$ µA mM^{-1} cm^{-2}, J_{max}=220.57 µA/cm^2). With lower (25 µg) or higher (100 µg and 150 µg) amounts of PPO/brushite cement, a marked drop of the sensitivity was observed (S= $1.02{\cdot}10^3$, $1.11{\cdot}10^3$ and $0.57{\cdot}10^3$ µA mM^{-1} cm^{-2} for 25, 100 and 150 µg respectively). The low sensitivity obtained with small film thickness can be clearly attributed to the low amount of enzyme used. Whereas if the layer thickness is increased as a consequence of adding high amounts of PPO/brushite, a diffusion barrier is formed hindering the access of the substrate to the enzyme and of the enzyme product to the electrode. The thickness obtained with 50 µg of mixture appears to be at the midpoint between these two effects, resulting in optimum analytical performance.

3.2.1.3. Time of cross-linking reaction with glutaraldehyde. When tyrosinase is simply adsorbed onto the brushite matrix, the enzyme is leaked off the surface to some extent during biosensor preparation [27]. Hence, a cross-linking process with glutaraldehyde is necessary to achieve effective immobilization of the enzyme within the matrix. This process is done through exposure of the electrode to GA vapor after enzyme adsorption. The effect of the cross-linking reaction time was investigated by adjusting the exposure time to GA vapor ranging between 5 and 25 min, after deposition of 50 µg of PPO/brushite mixture (1/1) on the GCE surface.

Maximum current and sensitivity increase as a function of the cross-linking time, up to the optimal value of 15 min (J_{max}=118.37 µA cm^{-2} and S=$0.40{\cdot}10^3$ µA mM^{-1} cm^{-2} for 5 min vs J_{max}=198.74 µA cm^{-2} and S=$1.43{\cdot}10^3$ µA mM^{-1} cm^{-2} for 15 min). Above this point, the response drops, i.e. approximately a 70% loss of sensitivity was evidenced ($0.59{\cdot}10^3$ µA mM^{-1} cm^{-2}). Full retention of the enzyme after 15 min and 25 min of cross-linking was verified by the absence of enzyme activity in the buffer solution used to stabilize the electrode. However, enzyme activity was observed with 5 min of time exposure. On the other hand, the sensitivity loss obtained with 25 min can indicate that long exposure times to GA can hinder the access of the substrate to active centers of tyrosinase and produce deactivation of these active centers due to an excess of unions between enzymes molecules. As a consequence, the biosensors used in the following studies were prepared with 15 min of GA exposure.

3.2.2. Optimization of the biosensor working conditions

The effect of potential, pH and temperature was investigated using a 1 mM tyramine solution, in the saturation domain. The influence of the applied potential on the biosensor response was checked in the range of −0.2 to +0.0 V. A bell-shaped profile was found, with the maximum response at −0.1 V. A slight decrease was observed at −0.05 V (94% of the maximum signal), higher at 0.0 V (40% of the maximum signal) and a pronounced decrease at more negative potentials (35% of signal at −0.2 V), that can be attributed to the electrode fouling produced by the polymerization of the enzymatically generated *o*-quinones at such negative potentials [32].

The influence of the pH on the biosensor response was investigated from pH 4.0–8.0, with tyramine 0.05 M in acetate/0.05 M phosphate buffer solutions. Once more, a bell shaped profile was obtained and the highest response was found at pH 6.0, which agrees with the optimum pH reported for the free enzyme [33]. At pHs 7 and 8 the response was reduced to 55% and 87% respectively. For low values of pH a drastic reduction was observed, 85% for pH 5.0 and no signal for pH 4.0. Therefore, all of the following experiences were carried out in PBS pH 6.0.

In the temperature study a range of 10–50 °C was tested, using 1 mM tyramine solution under oxygen saturation conditions to be sure that the oxygen concentration does not limit the rate of the reaction. The response increased gradually with the temperature (Fig. 5), reaching a maximum with 35 °C, followed by a high decrease (80%) when

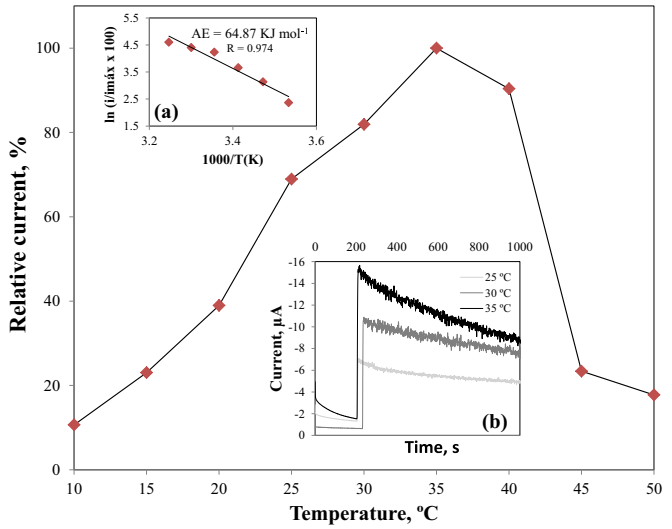

Fig. 5. Effect of temperature on the brushite cement biosensor response for 1 mM of tyramine in 0.1 M PBS pH 6.0. Inset (a): Arrhenius plot of tyrosinase immobilized in brushite cement with data in which enzyme is thermally stable. Inset (b): effect of temperature on response.

temperature was 45 °C. A study of thermal stability of the enzyme was performed to monitor biomolecule stability with time. For temperatures higher than 25 °C, a drastic decrease in the steady state current was observed. Thus, 25 °C was chosen as working temperature to avoid the eventual inactivation of tyrosinase. The Arrhenius plot for the enzyme immobilized in brushite cement shows a linear region with activation energy of 64.87 kJ mol^{-1}, a value much higher than that of PPO in solution, 17.6 kJ mol^{-1}.

Similar results occurred when glucose oxidase was immobilized in this material [28]. The evidence of only one linear region in the Arrhenius plot implies that there is no conformational changes in the enzyme in the temperature range studied, and also that the temperature did not affect the brushite matrix.

3.3. Biosensor behavior under optimal experimental conditions

The performance of the biosensor was tested under optimal conditions (50 µg of mixture enzyme-matrix, PPO/brushite ratio equal to 1.0, 15 min in GA vapor, pH 6.0 and 25 °C). The analytical properties of the biosensor are shown in Table 2. A linear relationship between the current signal and the tyramine concentration was obtained up to 16 µM, with a J_{max} of 282 µA cm^{-2} (Fig. 6). The corresponding regression equation was found to be I (mA) = 104.91 (± 5.82) [Tyramine] (M), R=0.9989 (n = 9). Table 2 also summarizes the characteristics of other biosensors for tyramine quantification. It must be emphasized that the method we propose for the fabrication of this biosensor is essentially a fast and easy method compared to others that require the synthesis of nanoparticles or sol-gel techniques. Moreover, this biosensor presents the lowest detection limit among previous reported.

3.4. Biosensor precision and stability

The repeatability of the biosensor has been checked by performing 10 successive amperometric measurements of 1 µM of tyramine using the same biosensor. Between measurements the biosensor was cleaned by rinsing with PBS 0.1 M. The relative standard deviation of the measurements was 6.5%. The intermediate precision was studied with the same biosensor in two different days, by 10 successive measurements, and the RSD value was found to be 7.2%, Reproducibility was evaluated by 5 successive measurements in three different biosensors, and a RSD value of 7.7% was obtained.

Table 2
Comparison of performances of different electrochemical biosensors for tyramine determination.

Immobilization system	Enzyme	Sensitivity	Linear range (M)	Detection limit (M)	Real samples	Reference
Adsorption in brushite + cross-linking with GA	Tyrosinase	15.0×10^2 mA $M^{-1}cm^{-2}$	5.8×10^{-7} to 1.6×10^{-5}	4.85×10^{-8}	Cheese	This work
Titania sol-gel modified with carbon materials and polymers	Tyrosinase	4.86×10^2 mA $M^{-1}cm^{-2}$	6.0×10^{-6} to 1.3×10^{-4}	1.5×10^{-6}	Cheese, sauerkraut and banana	[22]
Crosslinking in phosphate-doped polypyrrole film	Tyrosinase	1.07×10^2 mA M^{-1}	4.0×10^{-6} to 8.0×10^{-5}	5.47×10^{-7}	Sauerkraut	[24]
Carboxyl functionalized single-walled carbon nanotubes	Tyrosinase	59.0×10^2 mA M^{-1} cm^{-2}	5.0×10^{-6} to 1.8×10^{-4}	6.20×10^{-7}	Fish	[25]
MnO_2 and Nafion solution	Pea seedling amine oxidase	0.43 mA M^{-1}	1.0×10^{-5} to 3.0×10^{-4}	3×10^{-6}	Chicken meat	[34]
Epoxy resin membrane	Tyramine oxidase	–	1.8×10^{-5} to 2.5×10^{-4}	1.75×10^{-5}	Beer and sauce	[23]
Citric acid-capped silver nanoparticles	Tyramine oxidase	85.3 mA M^{-1} cm^{-2}	1.7×10^{-5} to 2.5×10^{-4}	1.0×10^{-5}	Beer and sauce	[26]
Nylon-net membrane	Diamine oxidase	–	1.0×10^{-6} to 5.0×10^{-5}	$5\ 10^{-7}$	Salted anchovy	[35]

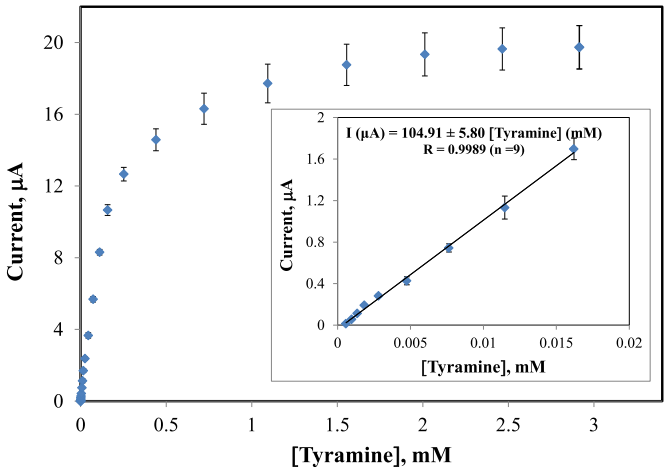

Fig. 6. (a) Calibration curve for tyramine under optimal conditions (PBS pH 6.0, 25 °C at −0.1 V vs. Ag/AgCl). Inset: Linear range of the calibration curve and amperometric responses of biosensor to successive additions of tyramine solution and biosensor response to tyramine. Errors bars from three different biosensors.

To investigate the stability, the biosensor was stored at +4 °C in 0.1 M PBS pH 6.0 and every day the amperometric response for 1 µM of tyramine was measured. The biosensor retained the 95% of the initial signal during 6 days and then a fast fall in the response (descent of 65% in the signal) was observed.

3.5. Interference study

Theoretically a device based on tyrosinase should be highly selectivity to tyramine detection because of the phenols oxidation involved in the enzyme reaction [36]. However, to assess the possible analytical application of the proposed sensor in the analysis of cheese, an interference study was conducted. The influence on the determination of tyramine of the amino acids and inorganic ions most abundant in this food was evaluated. The response of a 5 µM tyramine solution was compared with a 220-fold solution of glutamic acid and phenylalanine and a 900-fold tyrosine solution. The first amino acid studied was tyrosine, because of the similarity with tyramine in the chemical structure and its high concentration in cheeses.

Fig. 7A, shows the bell-shaped profiles obtained with a solution of tyramine 5 µM giving a very close signal at 0.1 and 0.05 V, 0.8 and 0.75 µA, respectively. Nevertheless, a marked decrease of the signal at these potentials was observed with a solution of tyrosine 4.5 mM (0.09 and 0.025 µA for −0.1 V and −0.05 V respectively). Glutamic acid and phenylalanine were also checked, but no signal was found in the range of the studied potentials.

Fig. 7B and C show the current response after additions of the above-considered amino acids. No significant changes in the current response was observed at −0.05 V.

Considering these results, and with the aim of preventing the interference caused by tyrosine, a compromise was found by carrying out the measure at a potential of −0.05 V.

Regarding inorganic ions, Mg^{2+}, Ca^{2+} and NO_3^-, were studied because their present in cheeses. When comparing the relative current response of a tyramine 10 µM solution without ions and with 50-fold ions, the signal did not show a significant increase (100 ± 8% tyramine free of inorganic ions and 104 ± 7%, 103 ± 8%, 107 ± 10% with Mg^{2+}, Ca^{2+} and NO_3^- respectively).

3.6. Biosensor application in real samples

Considering the high tyramine levels in aged cheeses [2,37] tyramine detection in Gouda and Brie cheeses was carried out with the brushite/PPO biosensor. After an appropriate pretreatment of these samples, the tyramine content in these types of cheeses was measured. Recovery studies were performed; the initial cheese samples were spiked with 75 mg of tyramine/ kg cheese. Good recoveries were obtained in an interval of 95.5–96.9% for both cheeses. The results, reflected in Table 3, indicate that the analytical method proposed here gave suitable responses for the samples used.

An increase in biogenic amines in foods can occur due to microbial

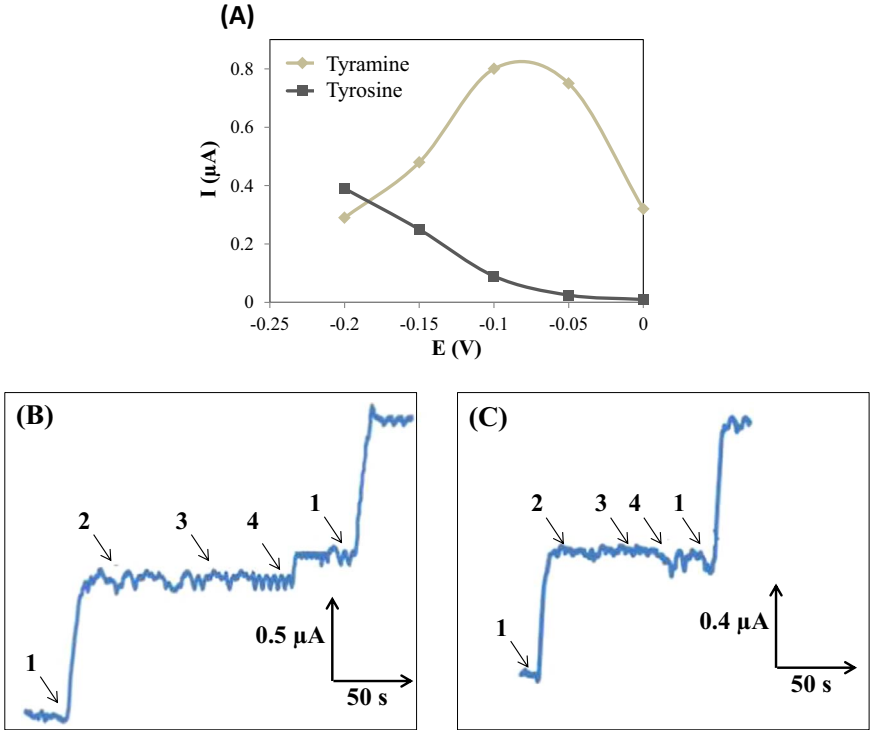

Fig. 7. Interference study. (A) Effect of the applied potential in the reduction current of tyramine and tyrosine. Amperometric Response to (1) tyramine 5 µM, (2) glutamic acid 1.1 mM, (3) phenylalanine 1.1 mM, and (4) tyrosine 4.5 mM, (B) at −0.1 V, (C) at −0.05 V. Experimental conditions: 0.1 M PBS pH 6.0 and 25 °C.

Table 3
Analytical recovery of added tyramine in the cheese samples.[a]

Real sample	Tyramine found in cheese sample (mg kg^{-1})	Tyramine added to cheese sample (mg kg^{-1})	Recovery (%)	RSD (%)
Gouda cheese	69.7 ± 4.9	75.0	95.5 ± 5.8	6.0
Brie cheese	29.8 ± 4.5	75.0	96.9 ± 7.5	7.7
Brie cheese[b]	31.3 ± 5.3	75.0	97.3 ± 8.2	8.4
Brie cheese[c]	59.0 ± 7.2	75.0	105.8 ± 8.4	7.9

[a] Average of three measurements.
[b] 3 days of storage at room temperature before measure.
[c] 7 days of storage at room temperature before measure.

contamination in inadequate conditions during storage. Thus, we carried out an analysis of Brie cheese after different days of storage. A piece of brie cheese was maintained at room temperature, and the tyramine content was determined after three and seven days. As shown in Table 3, the difference obtained in the first case was not significant ($p = 0.681$) but a 2-fold increase of tyramine concentration is obtained after a week of inadequate storage. This part of the study shows that this biosensor can be used for monitoring cheese degradation through tyramine determination.

4. Conclusions

In this work, electrochemical biosensors based on calcium phosphates as immobilization matrices for tyramine detection were proposed. These materials were selected considering their biocompatibility and protein adsorption capacity. The best analytical properties were obtained for brushite cement, revealing the importance of brushite crystal formation in the presence of tyrosinase in the biosensor performance. Brushite cement-PPO-GA based biosensor resulted in a highly sensitive, fast, inexpensive and easy analytical method for tyramine detection.

The analytical suitability of the proposed device was demonstrated by its application for tyramine detection in gouda and brie cheese. The recoveries obtained were in the range of 95.5–96.9%. The cheese tyramine content obtained over time showed the importance of monitoring the degradation of fermented dairy foods.

References

[1] S. Moret, D. Smela, T. Populin, L.S. Conte, A survey on free biogenic amine content of fresh and preserved vegetables, Food Chem. 89 (2005) 355–361.
[2] D.M. Linares, M.C. Martín, V. Ladero, M.A. Alvarez, M. Fernandez, Biogenic amines in dairy products, Crit. Rev. Food Sci. Nutr. 51 (2011) 691–703.
[3] European Comission Regulation (EC) No 2073/2005 of November 2005 on microbial criteria for foodstuffs.
[4] European Food Safety Authority Panel on Biological Hazards, Scientific opinion on risk based control of biogenic amine formation in fermented foods, EFSA J. 9 (2011) 2393.
[5] M. Fernandez, D. Linares, B. del Rio, V. Ladero, M.A. Alvarez, HPLC quantification of biogenic amines in cheeses: correlation with PCR-detection of tyramine-producing microorganisms, J. Dairy Res. 74 (2007) 276–282.
[6] O. Pinho, A. Pintado, A. Gomes, M. Pintado, F. Malcata, I. Ferreira, Interrelationships among microbiological, physicochemical and biochemical properties of Terrincho cheese, with emphasis on biogenic amines, J. Food Prot. 67 (2004) 2779–2785.
[7] E. Dadáková, M. Krízek, T. Pelikánová, Determination of biogenic amines in foods using ultra-performance liquid chromatography (ULPC), Food Chem. 116 (2009) 365–370.
[8] B. ten Brin, C. Damink, H.M. Joosten, J.H. Huis in´t Veld, Occurrence and formation of biologically active amines in foods, Int. J. Food Microbiol. 11 (1990) 73–84.
[9] R. Maijala, S. Eerola, Biogenic amines, in: H. Roginski, J. Fuquay, P. Fox (Eds.), Encyclopedia of Dairy Sciences, Elsevier Science, London, 2003, pp. 156–162.
[10] R. Burdychová, T. Komprda, Biogenic amine-forming microbial communities in cheese, FEMS Microbiol. Lett. 276 (2007) 149–156.
[11] R. Mercogliano, A. De Felice, C. Chirollo, M.L. Cortesi, Production of vasoactive amines during the ripening of Pecorino Carmasciano cheese, Vet. Res. Commun. 34 (2010) S175–S178.
[12] F. Galgano, G. Suzzi, F. Favati, M. Caruso, M. Martuscelli, M. Gardini, F. Salzano, G. Biogenic amines during ripening in "Semicotto Caprino" cheese: role of enterococci, Int. J. Food Sci. Technol. 36 (2001) 153–160.
[13] S. Novella-Rodriguez, M. Veciana-Nogués, A. Roig-Sagués, A. Trujillo-Mesa, M.C. Vidal-Carou, Comparison of biogenic amine profile in cheeses manufactured from fresh and stored (4 °C, 48 h) raw goat's milk, J. Food Prot. 67 (2004) 110–116.
[14] C. Ruiz-Capillas, F. Jimenez-Colmenero, Biogenic amines in meat and meat products, Crit. Rev. Food Sci. Nutr. 44 (2005) 489–499.
[15] M. Gil-Agustí, S. Carda-Broch, L.I. Monferrer-Pons, J. Esteve-Romero, Simultaneous determination of tyramine and tryptamine and their precursor amino acids by micellar liquid chromatography and pulsed amperometric detection in wines, J. Chromatogr. A 1156 (2007) 288–295.
[16] A. Önal, S.E.K. Tekkeli, C. Önal, A review of the liquid chromatographic methods for the determination of biogenic amines in foods, Food Chem. 138 (2013) 509–515.
[17] T. Chaves de Figueiredo, D.C. Sampaio de Assis, L.D. Miranda Menezes, G. Resende da Silva, I. Pereira Lanza, L.G. Dias Heneine, S. Vasconcelos Cançado, HPLC-UV method validation for the identification and quantification of bioactive amines in commercial eggs, Talanta 142 (2015) 240–245.
[18] A. Önal, A review: current analytical methods for the determination of biogenic amines in foods, Food Chem. 103 (2007) 1475–1486.
[19] L.M. Swann, S.L. Forbes, S.W. Lewis, A capillary electrophoresis method for the determination of selected biogenic amines and amino acids in mammalian decomposition fluid, Talanta 81 (2010) 1697–1702.
[20] V. Ladero, N. Martínez, M. Cruz Martín, M. Fernández, M.A. Alvarez, qPCR for quantitative detection of tyramine-producing bacteria in dairy products, Food Res. Int. 43 (2010) 289–295.
[21] M.R. Loizzo, F. Menichini, N. Picci, F. Puoci, U.G. Spizzirri, D. Restuccia, Technological aspects and analytical determination of biogenic amines in cheese, Trends Food Sci. Technol. 30 (2013) 38–55.
[22] J. Kochana, K. Wapiennik, P. Knihnicki, A. Pollap, P. Janus, M. Oszajca, P. Kustrowski, Mesoporous carbon-containing voltammetric biosensor for determination of tyramine in food products, Anal. Bioanal. Chem. 408 (2016) 5199–5210.
[23] S. Lata, S. Yadav, R. Bhardwaj, C.S. Pundir, Amperometric determination of tyramine in sauce and beer by epoxy resin biocomposite membrane bound tyramine oxidase, Sens. Instrum. Food Qual. Saf. 5 (2011) 104–110.
[24] I.M. Apetrei, C. Apetrei, Amperometric biosensor based on polypyrrole and tyrosinase for the detection of tyramine in food samples, Sens. Actuators B 178 (2013) 40–46.
[25] I.M. Apetrei, C. Apetrei, The biocomposite screen-printed biosensor based on immobilization of tyrosinase onto the carboxyl functionalized carbon nanotube for assaying tyramine in fish products, J. Food Eng. 149 (2015) 1–8.
[26] B. Batra, S. Lata, R. Devi, S. Yadav, C.S. Pundir, Fabrication of an amperometric tyramine biosensor based on immobilization of tyramine oxidase on AgNPs/ LCys-modifed electrode, J. Solid State Electron. 16 (2012) 3869–3876.
[27] M. Sánchez-Paniagua López, F. Tamimi, E. López-Cabarcos, B. López-Ruiz, Highly sensitive amperometric biosensor based on a biocompatible calcium phosphate cement, Biosens. Bioelectron. 24 (2009) 2574–2579.
[28] M. Sánchez-Paniagua López, B. López-Ruiz, A sensitive glucose biosensor based on brushite, a biocompatible cement, Electroanalysis 23 (2011) 280–286.
[29] D. Carelli, D. Centonze, C. Palermo, M. Quinto, T. Rotunno, An interference free amperometric biosensor for the detection of biogenic amines in food products, Biosens. Bioelectron. 23 (2007) 640–647.
[30] E.A. Cummings, S. Linquette-Mailley, P. Mailley, S. Cosnier, B.R. Eggins, E.T. McAdams, A comparison of amperometric screen-printed carbon electrodes and their application to the analysis of phenolic compounds present in beers, Talanta 55 (2001) 1015–1027.
[31] M. Sánchez-Paniagua López, B. López-Ruiz, Inhibition biosensor based on calcium phosphate materials for detection of benzoic acid in aqueous and organic media, Electroanalysis 23 (2011) 264–271.
[32] F. Liu, A.J. Reviejo, J.M. Pingarrón, J. Wang, Development of an amperometric biosensor for the determination of phenolic compounds in reversed micelles, Talanta 41 (1994) 455.
[33] R.S. Brown, K.B. Male, J.H.T. Luong, A substrate recycling assay for phenolic compounds using tyrosinase and NADH, Anal. Biochem. 222 (1994) 131–139.
[34] D. Telsnig, K. Kalcher, A. Leitner, A. Ortner, Design of an amperomeric biosensor for the determination of biogenic amines using screen printed carbon working electrodes, Electroanalysis 25 (2012) 47–50.
[35] R. Draisci, G. Volpe, L. Lucentini, A. Cecilia, R. Federico, G. Palleschi, Determination of biogenic amines with an electrochemical biosensor and its application to salted anchovies, Food Chem. 62 (1998) 225–232.
[36] A. Sánchez Ferrer, J.N. Rodríguez López, F. García Canovas, F. García Carmona, Tyrosinase. A comprehensive review of its mechanisms, Biochim. Biophys. Acta 1247 (1995) 1–11.
[37] N. Benkerroum, Biogenic amines in dairy products: origin, incidence and control means, Compr. Rev. Food Sci. Food Saf. 31 (2000) D37–D47.